Thermal Plasma Synthesis of Iron Oxide Aerosols and Their Characteristics

V. Subramanian, R. Baskaran*, H. Krishnan

Radiological Safety Division, Indira Gandhi Centre for Atomic Research, Kalpakkam, INDIA

Abstract

Thermal Plasma synthesis of Hematite Fe_2O_3 particles has been carried out for the generation of sub-micrometer range of particles. The plasma torch acts as a source of thermal energy and the plasma forming gas provides an inert atmosphere. The plasma column is stabilized by gas flow stabilization method in which a flowing external cold layer of a gas surrounds the arc column and the sheath gas enters into the reaction region. The sub-micrometer particles are generated by varying sheath gas with air and nitrogen, so that, the oxygen availability is varied during the formation of sub-micrometer particles. The plasma synthesized particles are characterized by X-ray diffraction, Moessbauer spectroscopy and spectrochemical analysis. The particle size distribution of the suspended aerosols and the aerosol deposits are determined. The aerosol size spectrum showed the presence of particles ranging from nano-meter to micrometer. Quantification of Fe^{2+} and Fe^{3+}present in the aerosol deposits showed that the generation of Fe^{2+} has been enhanced by 2% when the sheath gas is changed from air to nitrogen.

Keywords: Hematite; Aerosol characteristics; Fe^{2+} and Fe^{3+} states.

INTRODUCTION

Thermal Plasma Technology covers today a wide spectrum of applications (Pfender L.F, 2000), which are classified as (i) plasma coating including spraying, (ii) plasma chemical vapor deposition, (iii) plasma waste destruction, (iv) plasma densification of powders, (v) plasma metallurgy and, (vi) plasma synthesis of fine powders in generating nanometer particles. The high temperature (of the order of 10000 K) of the plasma state is utilized for the interaction of plasma with solids and gases, and this high temperature interaction is the basis for plasma-enabled material processing called as plasma synthesis (Young and Pfender, 1985). The plasma synthesis can also be carried out in an inert atmosphere. Therefore, pure metals or non oxides can be manufactured that are not

* Corresponding author: Tel: ++91+44 27480352;
Fax: ++91+44 27480216
E-mail address: rb@igcar.gov.in

available from other processes like flame synthesis. The fine particles are formed by plasma synthesis (Friedlander, 1998) by gas-to-particle conversion. Condensable molecules produced by this processes, self-nucleate to form particles.

Plasma synthesis is carried out using a Plasma Torch. The high temperatures together with the high reactivity due to the presence of free ions and radicals make the plasma a powerful medium to promote high heat transfer rates and chemical reaction. The materials introduced into the flame are melted and evaporated while plasma forming gas provides an inert atmosphere and helps to prevent undesirable reactions. The advantages of plasma torch in material processing (Sreekumar *et al.*, 2000; Venkataramani, 2002) include (i) high enthalpy to enhance the kinetics of the reaction, (ii) steep temperature gradient that enables rapid quenching and, (iii) the clean reaction atmosphere or varying the reaction atmosphere. These processes in tandem can produce a number of effects in material processing to produce high purity materials of ultra-fine powders (Einer Kruis *et al.*, 1998). In general, nitrogen or hydrogen is used as a plasma generating gas, since the energy content of nitrogen and hydrogen is higher than that of argon or helium, due to its diatomic nature. But, in order to have an inert atmosphere in the reaction environment, argon is usually preferred. Reactive gases like hydrogen, oxygen (air), chlorine and nitrogen can be used to impart reducing, oxidizing, chloriding or nitriding effects in the material processing. In the present experiment, reaction atmosphere is varied by changing the sheath gas used for the plasma torch as air and nitrogen so that oxygen availability is varied, and nano to submircometer range of particles are generated. By considering the multiple usage of iron-oxide powder in various industries (Bate, 1980; Matijevic *et al*., 1986) plasma synthesis of iron oxide powder is carried out.

Production of Iron oxide particles have been reported by the methods like (a) electrochemical synthesis, (b) laser pyrolysis, (c) wet chemical methods, (d) co-precipitation, (e) joule heating or exploding wire techniques and, (f) flame synthesis. In chemical preparative methods, the various parameters like pH, oxidative radicals, electro-chemical potential, Fe/lauric acid ratio etc. is critical in controlling the purity and morphology of iron oxide particles. The flame synthesis offers temperature upto 2000 K, which would results in improper melting of entire precursor powders within the short transit time, but this technique is widely used to produce carbon black, titanium dioxide and fume silica. The joule heating and exploding wire techniques are employed only in the case bulk materials to be used as a precursors and it is difficult to regulate the current density and other reactive environment. In plasma synthesis, plasma flame operates at temperature in excess of 10000K, which results in extremely fast chemical reaction and the products are volatile. The rapid cooling of reaction products leads to supersaturating and homogeneous nucleation.

Plasma synthesis of Iron oxide particles is reported by Balasubramanian *et al.* (2004) and

Banerji *et al.* (2006) using atmospheric transferred arc thermal plasma torch. Balasubramanian *et al*. in his studies, generated gamma Fe_3O_4 particles from the block of iron. By increasing arc current of the plasma, the author was able to increase the oxidation rate and generated gamma Fe_3O_4 particles. Banerjee *et al*. in his studies, enhanced the oxygen availability to 25% so as to increase the oxidation process to get gamma Fe_2O_3 particles. From these studies it is understood that the primary nucleation of Iron in the presence of Oxygen decides the formation of Fe_2O_3 or Fe_3O_4 particles. In our studies, the plasma synthesis of Fe_2O_3 particles is carried out in two different conditions i.e. (i) by keeping plasma generating gas as Nitrogen and the sheath gas as Air (sample S1) and (ii) by keeping plasma generating gas and the sheath gas as Nitrogen (sample S2), so as to vary the availability of oxygen while nucleation, and the fine particles are generated. The aerosol deposits generated by the above two methods were analyzed for the quantitative estimation of Fe^{2+} and Fe^{3+} by using spectrochemical analysis and verified using XRD and Moessbauer Spectroscopic methods. Besides, the suspended aerosols are characterized using various diagnostic equipments. All the results are reported in this paper.

EXPERIMENTAL

Aerosol Test Facility (ATF)

ATF (Baskaran *et al*., 2004; Baskaran *et al*., 2006) mainly consists of an aerosol chamber of volume one cubic meter, a plasma torch for the production of aerosols of fission products and fuel equivalent materials, a sodium combustion cell for the production of sodium aerosols (not been used for this experiments), aerosol measurement apparatus Mastersizer (Model: Mastersizer-S, M/s Malvern, UK), Low Pressure Impactor (LPI) (M/s Andersen Inc., USA), Aerosol Spectrometer with dilutor (Model 1.108 and Model 1.159 M/s Grimm Aerosoltech, GmbH, Germany), Filter paper sampler, humidity controller, auxiliary systems (water cooling, air flow, gas flow, pneumatic control, vacuum, material handling systems) and on-line data acquisition system for temperature, pressure and relative humidity (RH) during experiments. Aerosol measurement apparatus are connected to the chamber with the help of nozzles, which provide isokinetic sampling (William C. Hinds, 1982).An integrated view of aerosol chamber, the sodium combustion cell, and aerosol measurement apparatus is presented in Fig.1. The synthesis of iron oxide is carried out using the thermal plasma torch of the ATF.

Plasma Torch

The plasma torch is operated in non-transferred arc mode and it operates in atmospheric pressure. It has a rod type cathode, made of tungsten of 6 mm diameter with 1-2% of thoria for better thermionic emission (Baskaran *et al.*, 2004). The anode is made of copper, in the form of divergent nozzle with a conical shape, having 17 mm inner diameter and 75 mm outer diameter. Both the anode and cathode are water cooled and immersed in

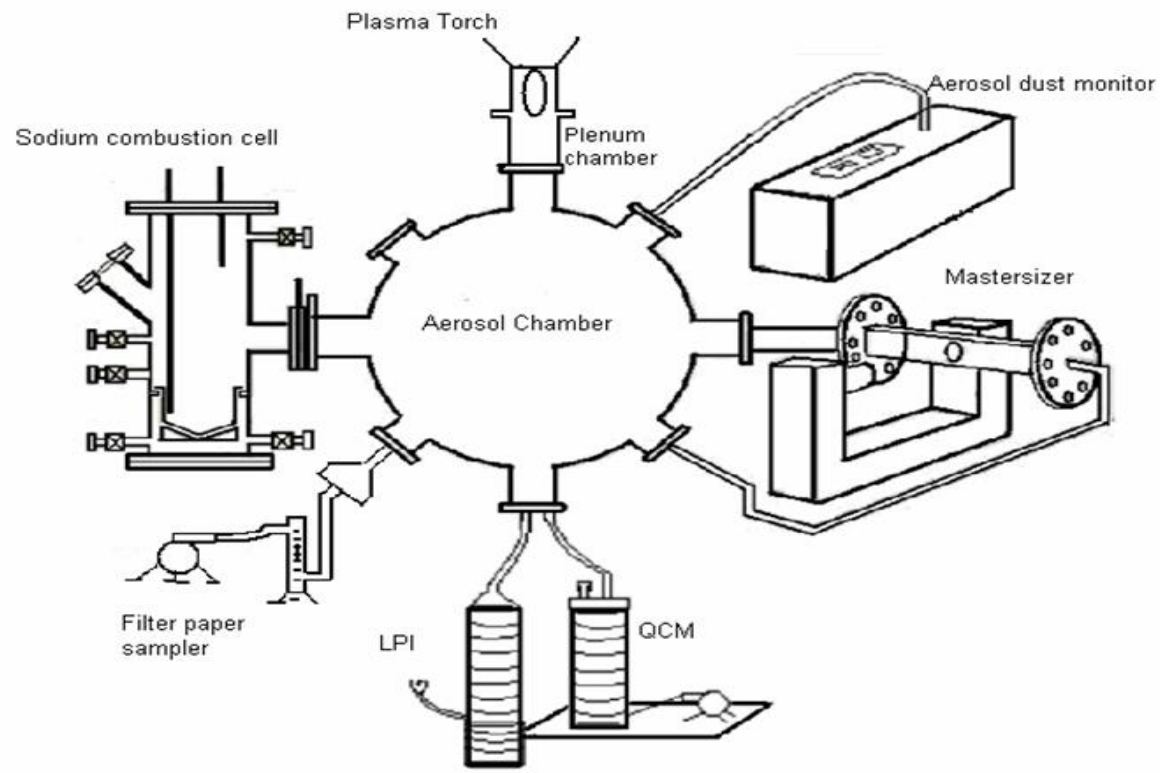

Fig. 1. A schematic of the ATF showing aerosol chamber, Plasma Torch and other aerosol diagnostic equipments.

an axial magnetic field for the stabilization of the arc. Magnetic coil is wound on nylon bobbin using 0.5 mm enameled copper wire of 450 turns. Typical current passed through is around 2 A. The magnetic field is produced parallel to both anode and cathode axis. The over all dimension of the torch is 82 mm. Nitrogen is used as plasma generating gas. The sheath gas used in plasma torch is either Nitrogen or Air. The plasma torch power supply consists of four different circuits namely, (1) High Voltage and High frequency generator (3kV-3MHz), (2) Magnetic coil supply (3) Three phase rectifiers and, (4) 12V DC supply for relays operation. Fig. 2 shows the schematic diagram of the torch and its accessories.

The arc is initiated between the cathode and auxiliary anode using a high voltage high frequency source and then transferred to copper anode. The arc route at the anode side was rotated by applying magnetic field. The plasma gas flow rate and the electric power to the torch are carefully metered to sustain the flow of arc. A typical arc is stabilized at a power of 20 kW with 50 Lpm gas flow rate for both plasma generating gas and sheath gas. Fig. 3 shows the photograph of the arc at a power of 20 kW. The typical arc length is about 450 mm.

Aerosol feed material is injected in to the plasma torch either by a powder feeder (M/s Metallizing Equipments, Model PF700, India) or by a wire feeder. The powder feeder

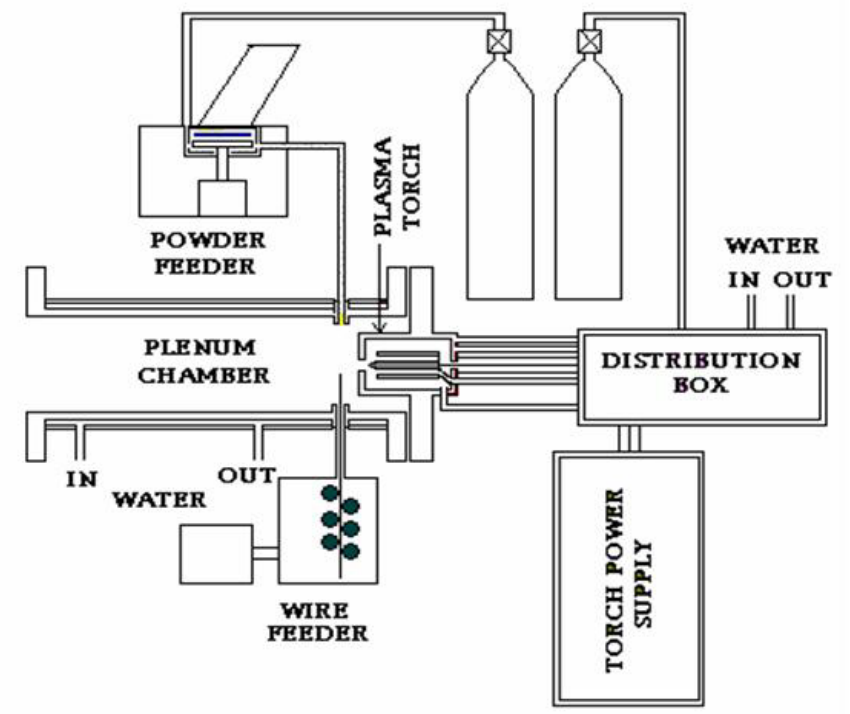

Fig. 2. A schematic diagram of the Plasma Torch and its accessories.

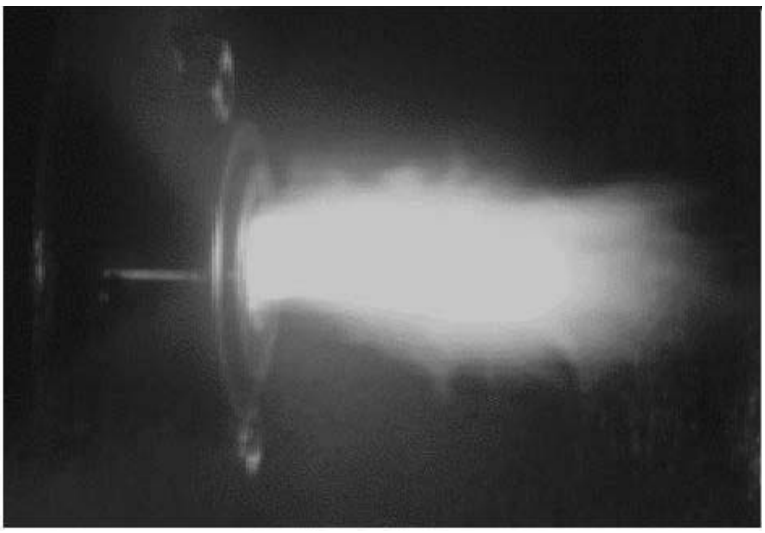

Fig. 3. A typical plasma arc photographed at the power 20 kW.

consists of a pressurized canister where the powder is kept and a slotted metal disc mounted off-centre with respect to canister. A given volume of powder fits into each slot of the disc and as disc rotates past the exit port; the carrier gas (Argon) passes through the disc carry the powder into the spray gun. The wire feeder has a stepper motor driving system, where the wire or a tube of 6 mm diameter, can be fed into the flame at the required rate. The mass flow of feed material Fe_2O_3 (Make: M/s Ranbaxy Chemicals, India) (primary particle size 40 μm) is calibrated as a function of carrier gas (Argon) flow rates and the

results are presented in the Fig 4. In order to achieve maximum efficiency in producing aerosols, the rate of powder injection has to be adjusted in tune with plasma gas flow rate. The carrier gas velocity (i.e the momentum imparted to the particles), the position of the powder injection nozzle (in our torch it is perpendicular to the plasma axis) and the Aspect ratio (Willike and Barib, 1993) (A) (A = L/D_j; L = 10 cm the distance between nozzle exit to the plasma axis and D_j = 0.8 cm diameter of powder jet nozzle) are important to get higher dwell time of the particles in the flame for the proper melting and evaporation of the materials (Solonenko, 2000). For the material in question, the velocity of the particles at the exit nozzle is found to be ~ 14 m/s (carrier gas flow rate 40 Lpm) for which the stopping distance (Hinds, 1982; Willike and Barib, 1993) is calculated to be ~36 cm. The powder is not dispersed at the exit nozzle but it flows as a stream of particles (stopping distance > L). As the exit nozzle is located perpendicular to the plasma axis on top of the anode, the material was found penetrating the plasma flame. As the plasma flow is strong enough, the major portion of the particles are carried away by the plasma flame (450 mm) and exit after the flame area.

RESULTS AND DISCUSSIONS

On-line Aerosol Characteristics

As plasma interaction is a high temperature interaction (of the order of 10000 K) followed by rapid quenching, the injected particles undergo phase changes, as well as there exist a possibility of structural changes in the compound (Gerdeman and Hecht, 1982). The torch was operated at 20 kW.

The primary particles were injected into the flame at the rate of 1 g/min. Aerosol sampling was carried out using Aerosol spectrometer, and 14 stage LPI (10 minutes sampling at a flow rate of 2.8 Lpm) connected to one of the diagnostic port of the aerosol chamber. The aerosol chamber was kept at the ambient atmosphere with RH at 65%. The on-line characteristics were carried out for the sample S1.

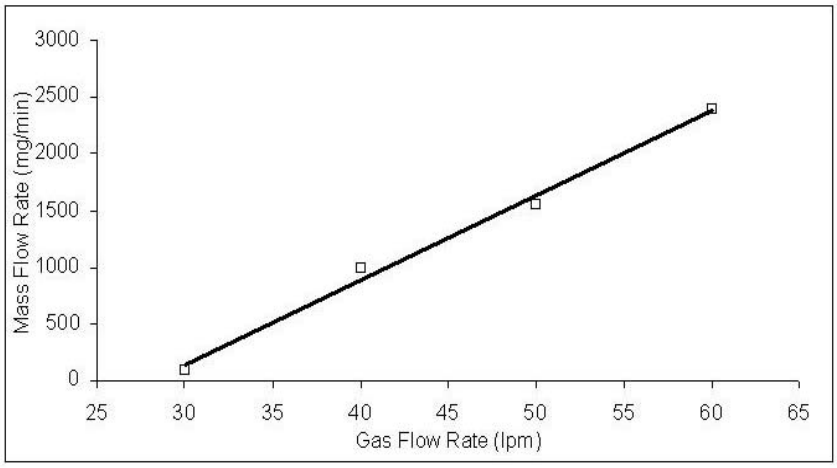

Fig. 4. Mass flow of feed material as a function of carrier gas flow.

The mass-size distributions measured by using LPI at various time delay (0, 60, 120 and 180 minutes) are shown in Fig. 5. The initial mass-size distribution is multimodal having open ended size range of particles below 0.1 μm and above 8.0 μm. It is observed from Fig. 5(a)-5(d), the particle size distribution found to vary with time due to coagulation and gravitational settling. It is to be noted from Fig. 5(a) that, the large quantity of mass is associated with small size range (0.09 μm = geometric mid point of the last two stages of LPI) of particles indicating the presence of large number of smaller size particles. It is further noticed that, from the LPI data of the Fig. 5(a), the aerosol mass collected on the filter stage (≤ 0.8 μm), is nearly 41.2% of the total mass. Gravitational coagulation is the dominating mechanism for the change of particle size distribution from Fig. 5(a)-5(d). The collision frequency between smaller and larger particles is very high which results in the reduction of tail in the lower size range in the distribution. The overall reduction of suspended mass fraction from Fig. 5(a)-5(d) is due to the gravitational

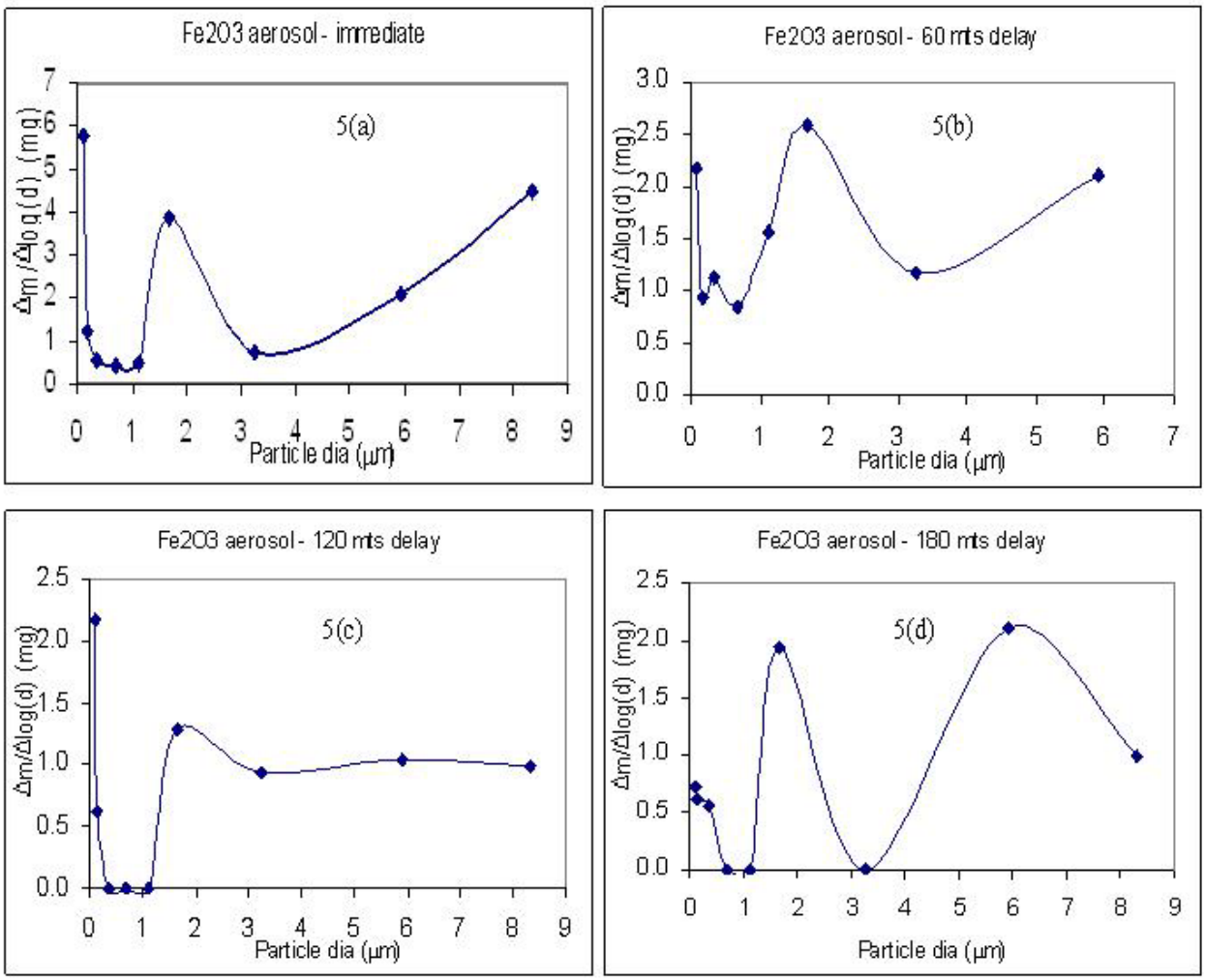

Fig. 5. Mass-Size distribution of suspended aerosol measured using LPI at various time.

settling of the coagulated larger particles. The presence of mode at different values (particle diameter) indicates the presence of various sized particles remain suspended at the time of sampling. However, it is also observed in all the figures that the submicron particles remain suspended even for longer time.

The aerosol spectrometer was operated in a sequential mode such that count-size distribution was measured every minute and stored. Fig. 6(a) shows the initial count-size distribution of aerosols measured during the first minute of injection of aerosols into the chamber and Fig. 6(b) shows the variation in number percentage of particles from first minute to fourth minute. It is observed from Fig. 6(a) that, as the peak value is heading towards the lower size ranges below 0.3 μm

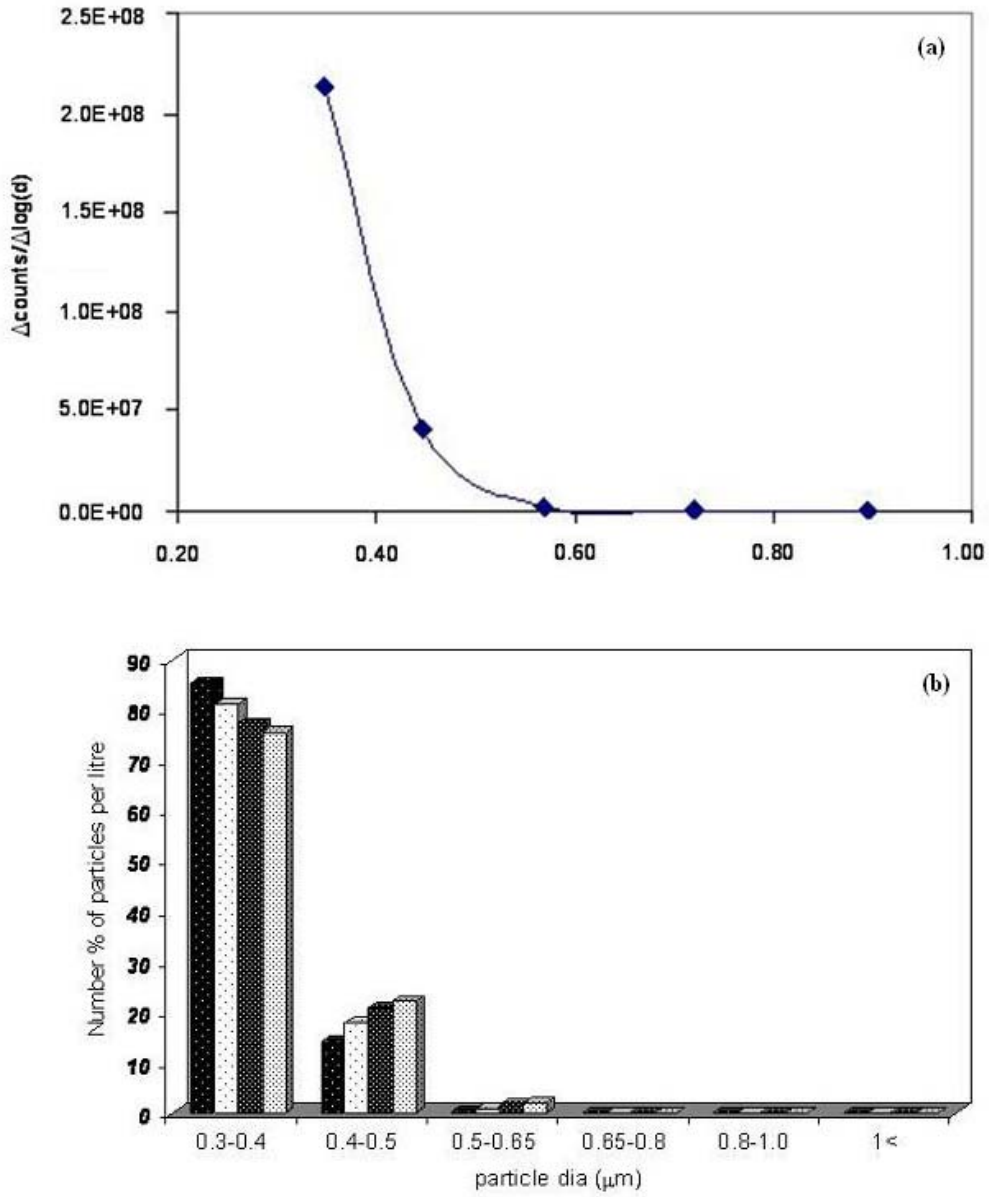

Fig. 6. (a) Count-size distribution of the particles measured during the first minute of the sampling, (b) Number % of particles Vs size for the duration 1-4 minutes.

(measurement limit of spectrometer) indicating the presence of large number of particles below 0.3 μm during the first minute of generation. It is noticed from Fig. 6(b) that, the particle size distribution found to vary with time due to coagulation. The analysis of aerosols size spectrum shows that the sub-micrometer to nano-size range of particles have been generated using the plasma torch.

Off-line Analysis of Aerosol Deposits

Analysis by Using Mastersizer

The particle deposits (sample S1) on the floor of the chamber was collected and analyzed in Mastersizer for the size spectrum. The Mastersizer operates in ensemble diffraction principle. The particles to be analyzed were made to disperse in a liquid medium (for iron oxide particles the dispersant is de-mineralized water) and made to intercept an optical path. The forward scattered intensity was recorded and the size spectrum was derived. The size spectrum of the particles deposited on the floor of the sample and primary particles are shown in Fig. 7. It is observed from the figure that the plasma synthesized particle spectrum is from 44 nm (lowest detection limit of the instrument) to 10μm. The median value of the primary particle spectrum is about 40 μm with standard deviation = 0.7.

SEM Analysis

The Scanning Electron Micrograph of the deposited particle for the sample S1 is shown in Fig. 8. It is observed that, there exist nearly spherical particle of about 2 μm, very fine individual particles in the sub-micrometer range and cluster aggregates. It is confirmed that the particle size distribution is wide as seen by the Mastersizer (Fig. 7).

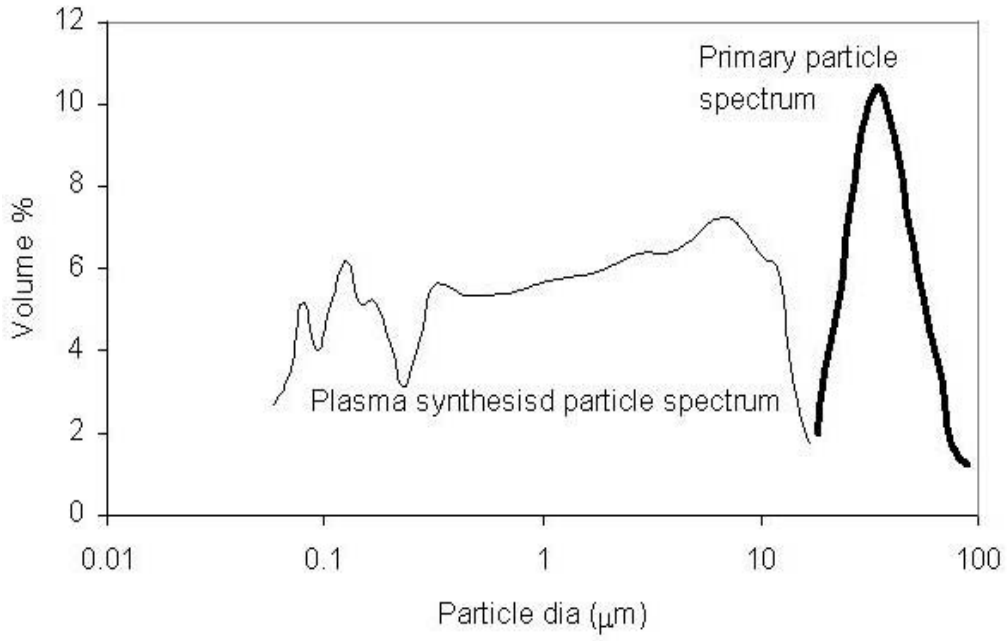

Fig. 7. Volume-size distribution of aerosol deposits on the floor measured using Mastersizer

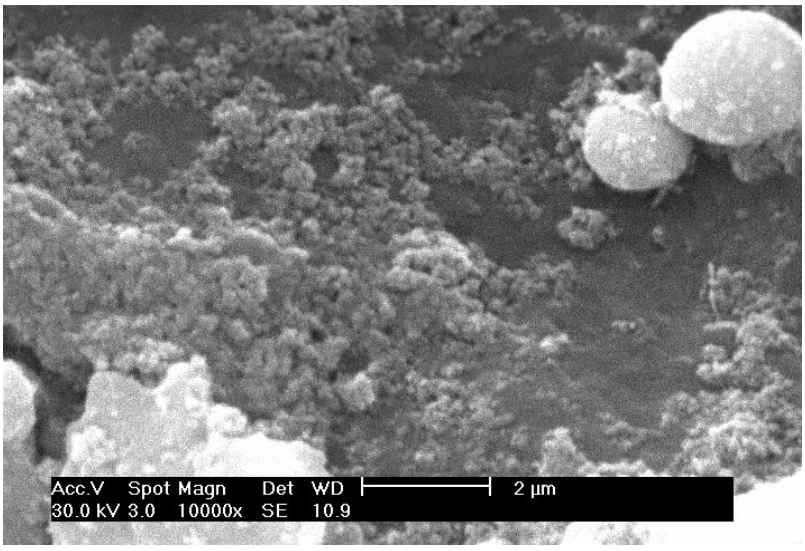

Fig. 8. Scanning Electron Micrograph of the sample S1.

XRD Analysis

The XRD pattern of the samples S1 and S2 are shown in Fig. 9(a) and Fig. 9(b) respectively. In both the patterns, it is observed that there is a presence of (i) α-Fe_2O_3 (rhombohedran), (ii) γ- Fe_2O_3 (Cubic) and, (iii) Cubic Fe_3O_4. The diffraction peak corresponds to FeO is not observed in the XRD pattern. In the plasma flame Hematite Fe_2O_3 is melted and evaporated. During the vapour to particle conversion phase, it forms combination of oxides of Iron in other phases (say Meghemite)and the diffusion of Fe^{2+} ion into the Maghemite structure resulting the formation of Cubic Fe_3O_4 (Magnetite) structure (Sung and Chung, 2006). Since it is difficult to quantify the composition of the aerosol deposits with respect to Fe_2O_3 and Fe_3O_4, using their relative intensity peaks vs. d space, in the XRD studies, the same particle deposits are analyzed using Moessbauer Spectroscopy and subjected to spectro-chemical analysis.

Moessbauer Spectroscopic Analysis

The Moessbauer spectrometer (M/s Wissel Instruments, Germany) is working in constant acceleration with transmission mode. ^{57}Co is used as a source, and velocity transducer is calibrated using by α-Fe (b.c.c) at room temperature. The measurement was carried out in room temperature. Fig. 10(a) and Fig. 10(b) are the Moessbauer spectrum (Greenwork N.N. and Gibb T.C, 1971) of the particle deposits, for the samples S1 and S2 respectively. The Moessbauer spectrum data is given in Table 1. It is observed from the Figures, there are three subspectra corresponding to two sextets indicating structurally different iron states, and one doublet. Two iron atoms are in magnetic environment and one in a paramagnetic environment. The sub spectrum 1 indicates the contribution by Fe^{3+} (tetrahedral). The sub spectrum 2 indicates the composition of Fe^{2+} and Fe^{3+} (octahedral) i.e. average of Fe^{2+} and Fe^{3+} (because of hopping). It is observed from the Table 1, that the isomer shifts for the

Sample S1 and Sample S2 at 0.65 mm/s and 0.85 mm/s respectively. The isomer shift and hyperfine value suggest that the phase is magnetite phase. The higher isomer shift for S2 indicates presence of more Fe^{2+} in the particles deposited under nitrogen atmosphere.

The single double-let observed in sub spectrum 3 indicates the presence of single domain particles (in the range of 10 nm). This is due to the collapse of hyperfine field caused by the faster relaxation rate than the Moessbauer life time (99.6 ns) by the particles

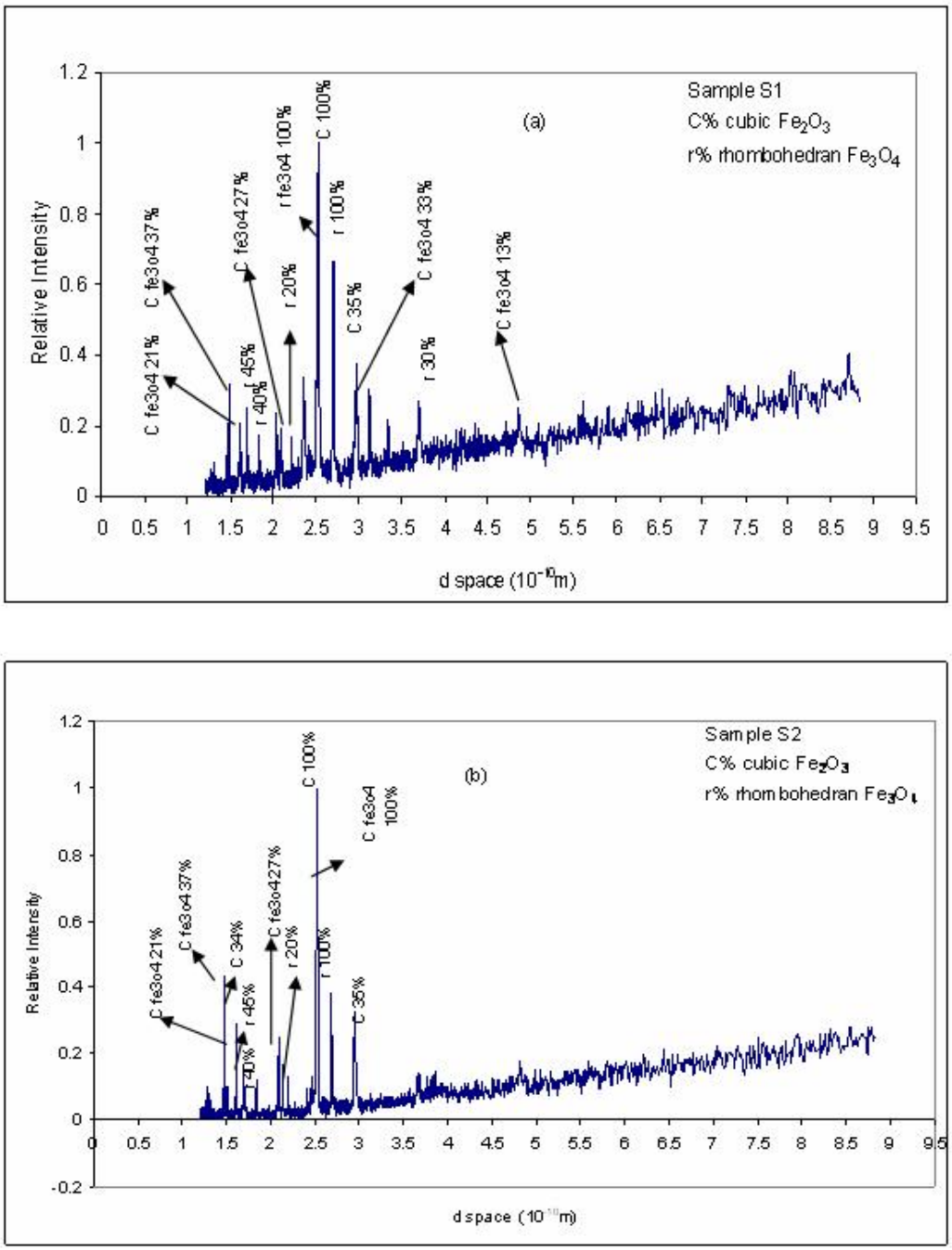

Fig. 9. XRD pattern of the aerosol deposits collected from the floor of the chamber (a) Sample S1 and (b) Sample S2.

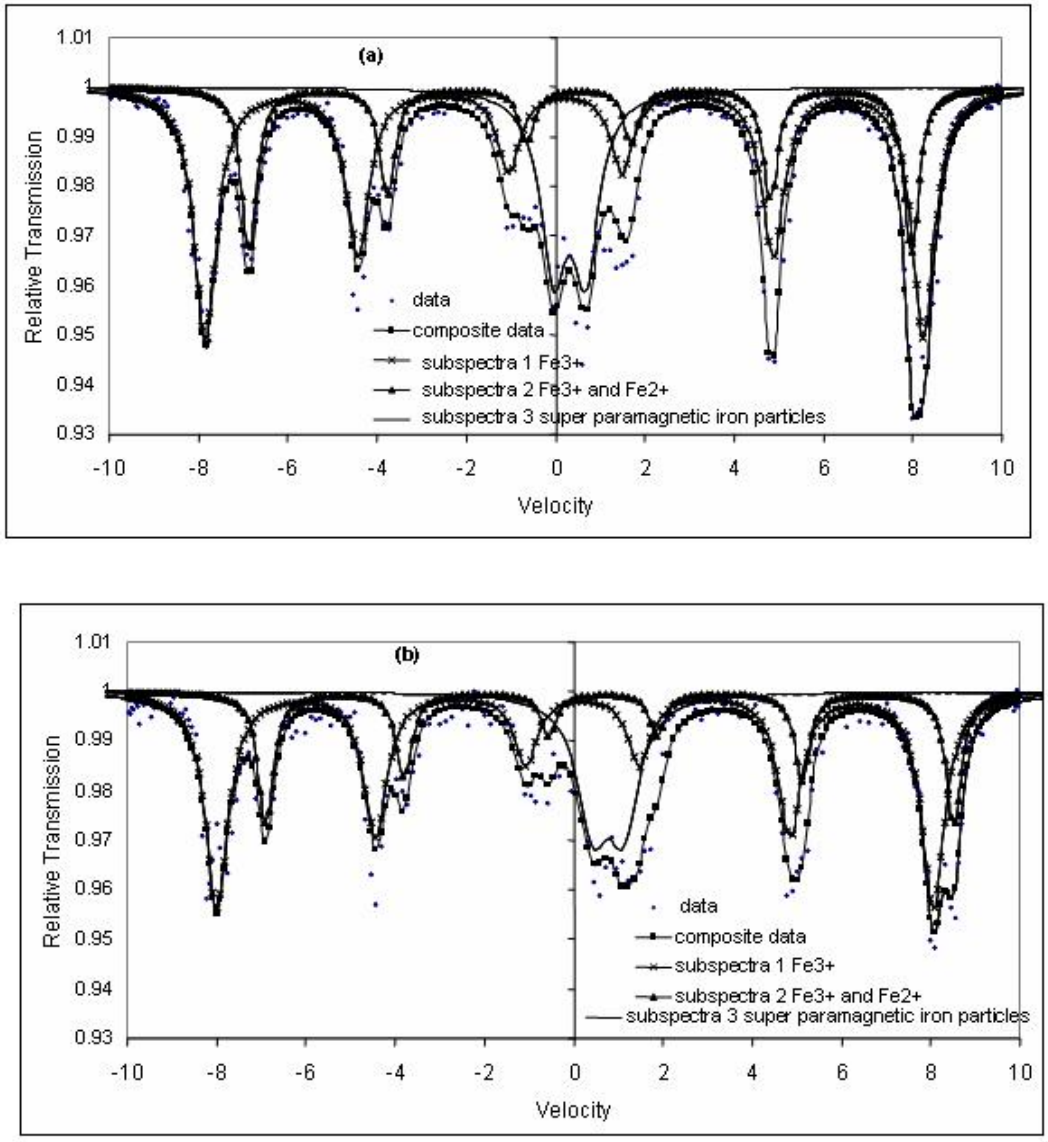

Fig. 10. Mossbauer Spectroscopic spectrum of the aerosol deposits collected from the floor (a) Sample S1; (b) Sample S2.

Table 1. Massbauer Spectroscopic data.

Sample		Isomershift (mm/s)	Hyperfine field (Tesla)	Quadrupole splitting (mm/s)	FWHM (mm/s)	Relative percentage
S1	Sub specta 1	0.32	49.87	-0.02	0.62	54.5
	Sub specta 2	0.65	45.99	-0.03	0.41	24.3
	Sub specta 3	0.41	-	0.71	0.69	21.2
S2	Sub specta 1	0.22	49.78	-0.17	0.62	55.8
	Sub specta 2	0.85	47.78	0.15	0.42	23.0
	Sub specta 3	0.87	-	0.68	0.82	21.2

Spectro-Chemical Analysis

The aerosol deposits collected during the experiments were analyzed for Fe^{2+} and Fe^{3+} using a reagent kit (Spectroquant, M/s.Merck, Germany) containing complexing agent (1,10-phenanthroline, Reagent Fe-1) , pH buffer (acetic acid + sodium acetate, Reagent Fe-2) and reducing agent (ascorbic acid, Reagent Fe-3). Hitachi-330 spectrophotometer was used for measuring the absorbance. The concentration of iron could be deduced from measured absorbance using the formula given below (http://photometrymerck.de).

Concentration of iron in mg/L = Absorbance × (0.06/0.01) (1)

The performance of the reagent kit was verified using standard of Fe^{2+} and Fe^{3+} solutions. About 4g of the aerosol deposits was digested with concentrated hydrochloric acid and evaporated to dryness. The residue was dissolved in double distilled water and the solution was made up to 50 ml in a standard flask (stock solution). This solution was further diluted to 16 times and to 8 ml of the diluted solution, 1 drop of Reagent Fe-1 and 0.5 ml of Reagent Fe-2 were added and pH of the resultant solution was adjusted to 3.5-4.0 using dilute sodium hydroxide solution. After 5 minutes, the absorbance of the solution was measured at 510 nm which corresponds to the concentration of Fe^{2+} present in the sample. Then, in the same sample, one dose of Reagent Fe-3 was added, shaken vigorously until the reagent was completely dissolved and left for 10 minutes. The measured absorbance at 510 nm corresponds to total iron concentration (Fe^{2+} + Fe^{3+}). The measured concentrations of Fe^{2+} and Fe^{3+} are given in Table 2. It is observed from the table that, the percentage of Fe^{2+} is increased from 5.11 to 7.06 from the sample S1 to S2; where as percentage of Fe^{3+} is reduced from 94.88 to 92.94. That is by keeping both plasma generating gas and sheath gas as nitrogen, improves the production of Fe^{2+} ion by 2%, that is the formation of Fe_3O_4 is enhanced by 2%. However, the total iron estimation of the two samples showed that, the total iron content remain same.

SUMMARY

The plasma torch is capable of producing aerosols in both sub-micrometer and nano-meter range of particles. Future experiments are planned to collect the size separated particles using Electrostatic precipitator and the magnetic properties will be studied. The versatile use of plasma torch in generating various compounds of Fe^{2+} or Fe^{3+} oxides is

Table 2. Results of Spectrochemical analysis of aerosol deposits.

Sample identity	Absor-bance due to Fe^{2+}	Conc. of Fe^{2+} (mg/L)	Absor-bance due to Fe^{2+} & Fe^{3+}	Conc. of Total iron (mg/L)	Conc. of Fe^{3+} (mg/L)	$\left[\frac{Fe^{2+}}{Fe_{tot}}\right]$ %	Total % of Iron
S1	0.03	0.18	0.586	3.516	3.336	5.11	70.067
S2	0.049	0.294	0.694	4.164	3.87	7.06	70.44

also explored by changing sheath gas used in the plasma torch. It is possible to enhance the production of Fe^{2+} by keeping the both plasma generating gas and sheath gas as nitrogen. Also it is possible to enhance the production of Fe^{3+} by keeping nitrogen as plasma generating gas and air as sheath gas. Thus reaction atmosphere has a key role in the formation of desired species. Further experiments are planned by keeping the aerosol chamber at the desired atmosphere for the production of Fe^{2+} or Fe^{3+} oxides.

ACKNOWLEDGEMENT

Facilitation Center for Industrial Plasma Technology, Institute for Plasma Research, Ahmedabad, India is acknowledged for the fabrication and supply of the plasma torch. Dr. G. Panneerselvam, Fuel Chemistry Division, IGCAR is acknowledged for XRD spectrographs. Shri P. Chandramohan and Dr. M.P. Srinivasan, Water and Steam Chemistry Laboratory, Bhabha Atomic Research Centre (BARC), Kalpakkam are acknowledged for Mossbauer spectroscopy. Dr. D. Ponraju, RSD, IGCAR is acknowledged for spectrochemical analysis. Mr.G.Partiban, RSD, IGCAR is acknowledged for the technical help during the experiments. Dr. R. Indira, Head, RSD, IGCAR is acknowledged for the helpful discussion during the experiment.

REFERENCES

Balasubramanian, C., Khollam, Y.B., Banerjee, I., Bakare, P.P., Date, S.K., Das, A.K. and Bhoraskar, S.V. (2004). DC Thermal Arc-plasma Preparation of Nanometric and Stoichiometric Spherical Magnetite (Fe_3O_4) Powders. *Mater. Lett.* 53: 3958-3962.

Banerjee, I., Khollam, Y.B., Balasubramanian, C., Pasricha, R., Bakare, P.P., Patil, K.R., Das, A.K. and Bhoraskar, S.V. (2006). Preparation of γ-Fe2O3 Nanoparticles Using DC Thermal Arc-plasma Route, Their Characterization and Magnetic Properties. *Scr. Mater*. 54: 1235-1240.

Baskaran, R., Selvakumaran, T.S. and Subramanian, V. (2004). Aerosol Test Facility for Fast Reactor Safety Studies. *Indian J. Pure Appl. Phys.* 42: 873.

Baskaran, R., Subramanian, V. and Selvakumaran, T.S. (2004). *Generation of Aerosols Using Thermal Plasma Torch for Fast Reactor Safety Studies.* IASTA Bulletin, 16, No. 1&2, p. 374.

Baskaran, R., Subramanian, V. and Selvakumaran, T.S. (2006*).* Real Time Measurement of Aerosol Size Distribution Using MASTERSIZER. *Indian J. Pure Appl. Phys.* 44: 576.

Bate, G., in: Wohlfarth E.D. (1980). *Ferromagnetic Material, Recording Materials Vol. 2*, North-Holland, Amsterdam.

Einer Kruis, F., Heinz Fissan and Aaron Peled. (1998). Synthesis of Nanoparticles in the Gas Phase for Electronic, Pptical and Magnetic Applications: A Review. *J. Aerosol Sci.* 29: 511-535.

Friedlander, S.K. (1998). *Synthesis of Nanoparticles and their Agglomerates:*

Aerosol Reactors, Chemical Engineering Department, UCLA, www.wtec.org/cgi.

Gerdeman, D.A. and Hecht, N.I. (1992). *Arc Plasma Technology in Material Science*, Springer Science, USA.

Greenwork, N.N. and Gibb, T.C. (1971). *Moessbauer Spectroscopy*, Chapman & Hall Ltd., India.

Hench, L.L. and Ulrich, D.B. (1986). *Colloid Science of Composite System, Science of Ceramic Chemical Processing*, Wiley, New York.

http://photmometry.merck.de Iron Test-100796. http://www.merck-chemicals.com/is-bin/INTERSHOP.enfinity/WFS/Merck-International-Site/en_US/-/USD/ViewProductDetail.

Pfender, L.F. (2000). Trends in Thermal Plasma Technology. *Thermal Plasma Torches and Technologies*. 1: 20-41.

Solonenko, O.P. (2000). Atmosphere Plasma Spraying: Theory, Modeling, Diagnostics, Computer-aided Design and Some Applications. *Thermal Plasma Torches and Technologies*. 1: 80-101.

Sreekumar, K.P, Ananthapadmanabhan, P.V., Venkaramani, N., Arshad Khan, Joshi, P.V., Sawant, V.D. and Mayya, Y.S. (2000). Aerosol Generation by Thermal Plasma Technique. *IASTA Bulletin*. 3: 110.

Sung, H.J. and Chung, I.F. (2006). *Nanotechnology for Environmental Remediation*, Springer, New York.

Venkataramani, N. (2002). Industrial Plasma Torches and Application. *Curr. Science*. 83: 254-262.

Willeke, K. and Barib, P.A. (1993). *Aerosol Measurement: Principles, Techniques and Applications*, Van Nostrand Reinhold, New York.

William, C.H. (1982). *Aerosol Technology*, John Wiley & Sons, USA.

Young, R.M. and Pfender, E. (1985). Generation and Behaviour of Fine Particles in Thermal Plasmas-A Review. *Plasma Chemistry and Plasma Processing.* 5: 1-37.

Received for review, March 3, 2008
Accepted, December 5, 2008